

# Chapter 11

## Boundary Shear Stress Distributions in Compound Channels Having Narrowing and Enlarging Floodplains



Kamalini Devi , Bhabani Shankar Das , Jnana Ranjan Khuntia ,  
and Kishanjit Kumar Khatua 

**Abstract** Compound channels are basically described as two stage open channels having main river and its adjoining floodplains. The momentum transfer phenomenon at the junction of main channel and floodplain is very crucial to be understood to estimate the discharge. The difference in water depth and roughness between the two zones generally causes momentum exchange at the interface. It is simple to quantify this momentum exchange for uniform flow conditions in river; however, for non-uniform flow condition the quantification is complex as the flow properties change in both longitudinal and lateral directions. Therefore, a study has been done on overbank flow with non-uniform flow condition, and stage discharge relationships are analyzed for accurate modeling. As natural rivers may have different configurations, so two different types of channels that are converging and diverging channels are considered and flow variables at different longitudinal positions are analyzed. Two discharge predicting models are developed which can be used for flow in natural rivers. These models depend on the non-dimensional forms of geometric and flow parameters and the percentage of the boundary shear forces carried by the adjacent floodplains. So it is required to analyze and estimate the boundary shear force distribution carried by main channel and non-prismatic floodplains before predicting flow. So, two different equations are proposed for percentage shear carried by converging and diverging floodplains. In addition, the developed models give simple ways for the quantification of percentage boundary shear force and provide accurate discharge result through non-prismatic channels. The predictions of the models are then compared with the

---

K. Devi (✉)

Department of Civil Engineering, Vidya Jyothi Institute of Technology, Hyderabad, Telangana 500075, India

B. S. Das

Department of Civil Engineering, National Institute of Technology, Bihar Patna 800005, India

J. R. Khuntia

Department of Civil Engineering, St. Martin's Engineering College, Dhulapally, Secunderabad, Telangana 500100, India

K. K. Khatua

Department of Civil Engineering, National Institute of Technology, Rourkela, Odisha 769008, India

models of other researchers. The prediction efficiency of the present model is found better than the models of previous researchers.

**Keywords** Momentum exchange · Non-uniform flow · Diverging floodplain · Converging floodplains · Stage-discharge relationships

## 11.1 Introduction

Compound channels are the typical patterns of flooded rivers. The study of these channels have become vital for environmental, ecological, and design issues. The behavior of flow in rivers for both in bank and overbank flow conditions have been widely investigated. It is found that many investigators have done their research under uniform flow conditions; however, in natural rivers the flow pattern is generally non-uniform flow. So the applications of models which are developed for uniform flow conditions are found to give spurious results for non-uniform flow conditions. For practical point of view, the uniform flow condition in a flooded river channel is ideal and is considered as a theoretical reference flow as stated by Proust (2005). So understanding and analyzing the non-uniform flow in compound channels become a universal research area nowadays. Bousmar and Zech (1999), Bousmar et al. (2004), Rezaei (2006), Proust et al. (2006), and Rezaei and Knight (2009) have analyzed the non-uniform flow in laboratory flumes. In laboratory environments, diverging and converging channels constructed as non-uniform flow are usually acquired in these types of non-prismatic compound channels. It is proved by many investigators that momentum transfer at junction of main channel and floodplain causes non-uniformity of the boundary shear stress distribution along the subsection perimeters. Moreover, the distribution of boundary shear force in subsections is also indispensable for investigating the sediment transport problems. Knight and Hamed (1984), Khatua et al. (2012), Mohanty et al. (2014), Devi et al. (2017), Khuntia et al. (2018) and Devi and Khatua (2020) developed models for distribution of boundary shear force for compound channels with homogeneous and non-homogeneous roughness by incorporating the momentum exchanges at junctions. For non-prismatic compound channels, Naik et al. (2017) developed a relationship to estimate percentage boundary shear force carried by floodplains of a converging compound channel as a function of geometric and hydraulic parameters. However, for diverging floodplains, there is less work found on lateral boundary shear distribution as well as on percentage shear force carried by floodplains (Das et al. 2020). Here, models are developed for percentage boundary shear force distribution in converging and diverging compound channels as a function of different geometric and hydraulic parameters of non-prismatic compound channels. Further, this distribution of boundary shear force is related to find out the discharge through the channels.

## 11.2 Experimental Setup

In this paper, the non-uniform steady flows are considered to be occurred in non-prismatic compound channels with narrowing and enlarging floodplains. The non-uniform steady flows are also occurred in prismatic geometries (Proust et al. 2013). Due to less availability of data sets, this type of flow condition is not considered here. In present research, two non-uniform flow geometric channels are considered. Firstly narrowing compound channels, where the upstream geometry gets reduced toward downstream as shown in Fig. 11.1a and second one is enlarging one where the upstream geometry gets enlarged along flow direction (Fig. 11.1b).

There are many investigations devoted for the modeling of boundary shear distribution in subsections of a compound channels under uniform flow condition (Khatua et al. 2011; Mohanty and Khatua 2014). As the cross section of a non-prismatic compound channel changes with the longitudinal distance, the flow depth varies in longitudinal direction. In a consequence, the distributions of the flow variables such as boundary shear and discharge vary longitudinally although the discharge remains constant. To study the variation, experiments are performed inside the flume having dimensions as 22 m long  $\times$  2 m wide  $\times$  0.5 m depth, for different geometric and hydraulic conditions. Three sets of experiments are conducted in compound channels having enlarging floodplains (enlarging angle  $5.93^\circ$ ,  $9.83^\circ$ , and  $14.57^\circ$ ) with six different relative flow depths (0.15, 0.20, 0.25, 0.30, 0.40, and 0.50). In this study, the available experimental data sets of previous investigators (both narrowing and enlarging compound channels) along with the data sets of own experimental channels are utilized (Das et al. 2019). The exchange of momentum at the interface between the main channel and the floodplains also strongly affects both boundary shear and velocity distribution.

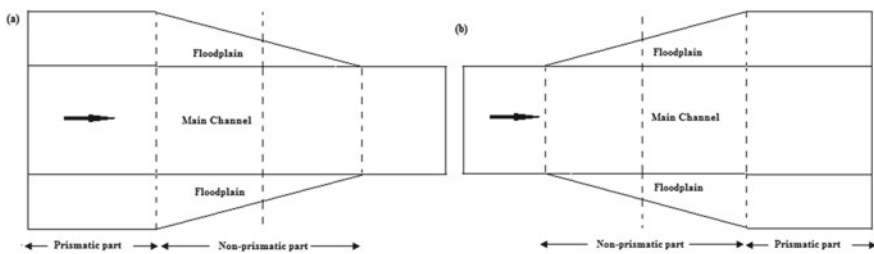


**Fig. 11.1** Top view of the compound channels with **a** narrowing geometries and **b** enlarging geometries

### 11.3 Preliminary Analysis

#### 11.3.1 Development of Boundary Shear Distribution Model

The boundary shear distributions for symmetric and asymmetrical straight compound channels are developed early by previous investigators. Figure 11.2 demonstrates the boundary elements of an overbank flow section. Boundary elements from *a* to *g* comprising the wetted perimeter denotes inclined floodplain wall of length  $\sqrt{2}(H - h)$ , left flood plain of width  $b_{f1}$ , main channel left side slope  $\sqrt{2}h$ , bed width of channel  $b$ , main channel right side slope  $\sqrt{2}h$ , right flood plain width  $b_{f2}$ , flood plain wall of inclined length  $\sqrt{2}(H - h)$  (Devi et al.). To estimate the shear force distribution (per meter length) at each element of the wetted perimeter, shear stresses at each point of the respective element are numerically integrated. To obtain the total shear force (per unit length of the wetted perimeter) of the compound channel, shear forces carried by all the elements are added. This is the total resistance offered by the compound channel, and it is used as a divisor while calculating percentage shear force carried by the flood plain  $\%S_{fp}$  or by other boundary elements.

Previous investigators have developed some equations for calculating  $\%S_{fp}$  as listed below.

1. Knight and Demetriou (1983)

$$\%S_{fp} = 48(\alpha - 0.8)^{0.289}(2\beta)^m \tag{11.1a}$$

2. Knight and Hamed (1984)

$$\%S_{fp} = 48(\alpha - 0.8)^{0.289}(2\beta)^m \left\{ 1 + 1.02\sqrt{\beta}\log\gamma \right\} \tag{11.1b}$$

The exponent *m* can be evaluated from the relation

$$m = 1/[0.75e^{0.38\alpha}] \tag{11.1c}$$

$\gamma$  is the ratio of roughness between flood plain and main channel.

3. Khatua and Patra (2007)

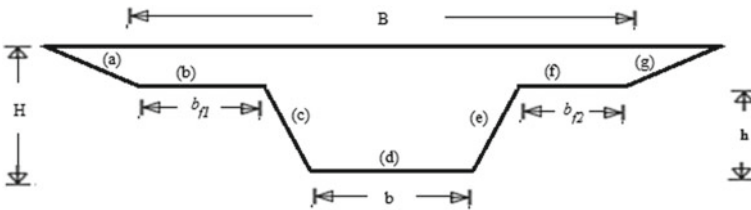


Fig. 11.2 Schematic cross section of symmetrical compound channel

$$\%S_{fp} = 1.23(\beta)^{0.1833}(38Ln\alpha + 3.6262) \left\{ 1 + 1.02\sqrt{\beta}\log\gamma \right\} \quad (11.1d)$$

4. Khatua et al. (2012)

$$\%S_{fp} = 4.1045 \left( \frac{100\beta(\alpha - 1)}{1 + \beta(\alpha - 1)} \right)^{0.6917} \quad (11.1e)$$

5. Mohanty et al. (2013)

$$\%S_{fp} = 3.3254 \left( \frac{100\{\beta\alpha\delta - \beta(\delta + 2s)\}}{\beta\alpha\delta + (1 - \beta)(\delta + s)} \right)^{0.7467} \left\{ 1 + 1.02\sqrt{\beta}\log\gamma \right\} \quad (11.1f)$$

Devi et al. (2016) found that expressions from (11.1a) to (11.1f) are well fitting to symmetric compound channels only. So, they developed a generalized relationship between  $\%S_{fp}$  and  $\%A_{fp}$  for asymmetrical compound channel as

$$\%S_{fp} = 3.576 \left\{ \frac{100\beta\left(\alpha - 1 - \frac{2.5s}{\delta} + \frac{0.5s}{\delta^*}\right)}{\left(1 + \frac{s}{\delta^*}\right) + \beta\left(\alpha - 1 - \frac{2s}{\delta}\right)} \right\}^{0.717} \quad (11.1g)$$

where width ratio ( $\alpha$ ) = (B/b), relative flow depth ( $\beta$ ) = (H - h)/H, main channel aspect ratio ( $\delta$ ) = (b/h), flow aspect ratio ( $\delta^*$ ) = (b/H), B = Total compound channel width, b = main channel bottom width, H = flow depth over main channel, h = bank full depth and for trapezoidal channel (V:H::l:s) s = side slope of main channel.

All the discussed models are suitable for straight compound channels having different cross-sectional geometries under uniform flow condition. However, for non-uniform flow condition, Naik et al. (2017) gave a boundary shear force model which is well fitted for compound channels having converging floodplains for limited flow and geometric condition only. According to the author’s knowledge, there has been a less work devoted to diverging compound channel and no suitable model has been developed for boundary shear force distribution for this type of channels. Keeping these points in view, this research has been extended to develop a general equation to predict boundary shear distribution for compound channels having non-prismatic floodplains. So, both converging and diverging compound channels are taken into account and separate models are proposed for each of them. For this purpose, experiments have been conducted and additional data sets have been collected from literatures.

For developing a model for any flow variable, the primary task is to make the dependent flow variable as non-dimensional. So, shear force distribution in terms of percentage shear force carried by floodplain ( $\%S_{fp}$ ) is made non-dimensional and taken as dependent flow variable. For both converging and diverging compound channels, percentage shear force carried by floodplain ( $\%S_{fp}$ ) is analyzed with dimensionless geometric and hydraulic parameters. The geometric and hydraulic parameters are selected investigating their dependencies on the percentage shear

force on floodplain ( $\%S_{fp}$ ). Width ratio, relative flow depth, flow aspect ratio ( $\delta^*$ ), relative longitudinal distance ( $X_r$ ), Reynolds no ( $Re$ ), and Froude's no ( $Fr$ ) are taken as the non-dimensional independent parameters which are influencing the shear force of non-prismatic compound channels. Width ratio ( $\alpha$ ) is defined as the ratio of the total width of compound channel to bottom width of the main channel, relative flow depth ( $\beta$ ) is defined as the ratio between the flow depth over floodplain ( $h$ ) to the total flow depth over main channel ( $H$ ), relative longitudinal distance ( $X_r$ ) is the ratio between the distance ( $l$ ) of a arbitrary reach of the non-prismatic reach in longitudinal direction to the total length ( $L$ ) of the non-prismatic reach. Flow aspect ratio ( $\delta^*$ ) is the ratio between the main channel bed width to the flow depth over it (Devi and Khatua 2019). As the behavior of flow in converging and diverging compound channels is notably different as investigated by previous researchers, so it needs to model the percentage shear force on floodplain ( $\%S_{fp}$ ) individually for these channels.

For developing the models of  $\%S_{fp}$ , converging and diverging experimental data sets from previous investigations are considered here and the details of their geometric, hydraulic, and roughness parameters are tabulated in Tables 11.1 and 11.2 (Das and Khatua 2017). Based on the experimental results of large numbers

**Table 11.1** Details of geometric parameters for all types of channel collected from experimental work and published data for diverging and converging compound channel (Das and Khatua 2018)

Verified test channel	$S_0$	$b$ in (m)	$h$ in (m)	$\theta$ in ( $^\circ$ )	A	$\delta$
1	2	3	4	6	5	7
NITR data-Dv5.93	0.0014	0.34	0.113	5.93	5.82–2.76	3.01
NITR data-Dv9.83	0.0014	0.34	0.113	9.83	5.82–2.76	3.01
NITR data-Dv14.57	0.0014	0.34	0.113	14.57	5.82–2.76	3.01
B et al.-Dv3.81	0.00099	0.40	0.05	3.81	3.0–1.0	8.00
B et al.-Dv5.71	0.00099	0.40	0.05	5.71	3.0–1.0	8.00
Y-Dv3.81	0.00088	0.40	0.18	3.81	3.0–1.0	2.22
Y-Dv5.71	0.00088	0.40	0.18	5.71	3.0–1.0	2.22
Y-Dv11.31	0.00088	0.40	0.18	11.31	3.0–1.0	2.22
NK-Cv5	0.0011	0.50	0.10	5.00	1.0–1.8	5.00
NK-Cv9	0.0011	0.50	0.10	9.00	1.0–1.8	5.00
NK-Cv12.38	0.0011	0.50	0.10	12.38	1.0–1.8	5.00
B-Cv3.81	0.00099	0.40	0.05	3.81	1.0–3.0	8.00
B-Cv11.31	0.00099	0.40	0.05	11.31	1.0–3.0	8.00
R-Cv1.91	0.002003	0.398	0.05	1.91	1.0–3.0	7.96
R-Cv3.81	0.002003	0.398	0.05	3.81	1.0–3.0	7.96
R-Cv11.31	0.002003	0.398	0.05	11.31	1.0–3.0	7.96

B et al.—Bousmar et al. (2004), Y—Yonesi et al (2013), NK—Naik and Khatua (2016), B—Bousmar (2002), R—Rezaei (2006), Longitudinal slope- $S_0$ , Main channel width in meter— $b$ , Main channel depth in meter— $h$ , Diverging angle in degree— $\theta$ , Width ratio— $\delta$ , Aspect ratio— $\delta$

**Table 11.2** Details of hydraulic and surface parameters for all types of channel collected from experimental work and published data for diverging and converging compound channel (Das and Khatua 2018; Das et al. 2019)

Verified test channel	$Q$ in (m <sup>3</sup> /s)	$N$	$\beta$	$Re$ in ( $\times 10^5$ )	$Fr$
1	2	3	5	6	7
NITR data-Dv5.93	0.026–0.067	0.0095–0.0161	0.146–0.51	0.49–1.58	0.42–0.68
NITR data-Dv9.83	0.025–0.065	0.0093–0.015	0.144–0.52	0.53–1.61	0.44–0.70
NITR data-Dv14.57	0.024–0.062	0.0087–0.0136	0.142–0.51	0.58–1.93	0.51–0.82
B et al.-Dv3.81	0.012–0.020	0.0053–0.025	0.218–0.51	0.34–1.39	0.38–0.86
B et al.-Dv5.71	0.012–0.020	0.0076–0.027	0.253–0.54	0.34–1.30	0.25–0.66
Y-Dv3.81	0.037–0.0615	0.0121–0.0211	0.142–0.36	1.43–1.93	0.24–0.33
Y-Dv5.71	0.037–0.0615	0.0129–0.0207	0.142–0.35	1.35–1.85	0.26–0.362
Y-Dv11.31	0.037–0.0615	0.0122–0.0223	0.143–0.35	1.28–1.74	0.28–0.38
NK-Cv5	0.043–0.062	0.010–0.014	0.15–0.30	0.47–1.46	0.64–0.83
NK-Cv9	0.042–0.059	0.012–0.0163	0.15–0.30	0.40–1.61	0.56–0.76
NK-Cv12.38	0.040–0.054	0.011–0.0176	0.15–0.30	0.50–1.73	0.58–0.70
B-Cv3.81	0.010–0.020	0.0087–0.0226	0.213–0.53	0.33–1.32	0.26–0.60
B-Cv11.31	0.010–0.020	0.009–0.0341	0.18–0.53	0.28–1.31	0.29–0.58
R-Cv1.91	0.015–0.040	0.0083–0.0141	0.18–0.52	0.42–1.45	0.56–0.81
R-Cv3.81	0.014–0.025	0.0093–0.0196	0.15–0.50	0.38–1.81	0.35–0.71
R-Cv11.31	0.013–0.023	0.0097–0.0183	0.19–0.50	0.42–1.92	0.38–0.76

B et al.—Bousmar et al. (2004), Y—Yonesi et al (2013), NK—Naik and Khatua (2016), B—Bousmar (2002), R—Rezaei (2006), Observed discharge in m<sup>3</sup>/s— $Q$ , Manning’s roughness coefficient— $n$ , Relative depth— $\beta$ , Reynolds number— $Re$ , Froude number— $Fr$

of published data sets, two individual equations are proposed for converging and diverging compound channel.

The most important task in developing the new boundary shear distribution model is to find out the most significant parameters controlling the boundary shear force distribution in compound channels. Due to the inherent variability of flow caused by interaction mechanism in compound channel, a large numbers of independent parameters may influence the boundary shear distribution. Hence, it makes difficulties in deriving the functional relationships between boundary shear forces with the independent parameters. The  $\%S_{fp}$  is primarily depending on the width ratio ( $\alpha$ ), relative flow depth ( $\beta$ ), and flow aspect ratio. In addition with these three non-dimensional parameters, three other influencing parameters, i.e., Reynolds number ( $Re$ ), Froude number ( $Fr$ ), and relative longitudinal distance ( $X_r$ ) are considered for development of the  $\%S_{fp}$  model for non-prismatic compound channels. So,  $\%S_{fp}$  may be functionally defined as

$$\%S_{fp} = F(\alpha, \beta, \delta^*, Re, Fr, X_r) \tag{11.2}$$

Figures 11.3, 11.4, 11.5, 11.6, 11.7, and 11.8 graphically presents the variation of  $\%S_{fp}$  value with relative flow depth, width ratio, flow aspect ratio, Reynolds number, Froude number, and relative longitudinal distance, respectively, for converging compound channel. The functional relationships that are existing between the  $\%S_{fp}$  with  $\alpha, \beta, \delta^*, Re, Fr, X_r$  are linear, exponential, logarithmic, power, logarithmic, and linear, respectively, for all converging compound channel considered.

Similarly for all the diverging compound channels the variations between the dependent parameter  $\%S_{fp}$  with the non-dimensional independent parameter are analyzed. The best relationships between  $\%S_{fp}$  and  $\alpha, \beta, \delta^*, Re, Fr, X_r$  are shown in Figs. 11.9, 11.10, 11.11, 11.12, 11.13, and 11.14. The functional relationships that are

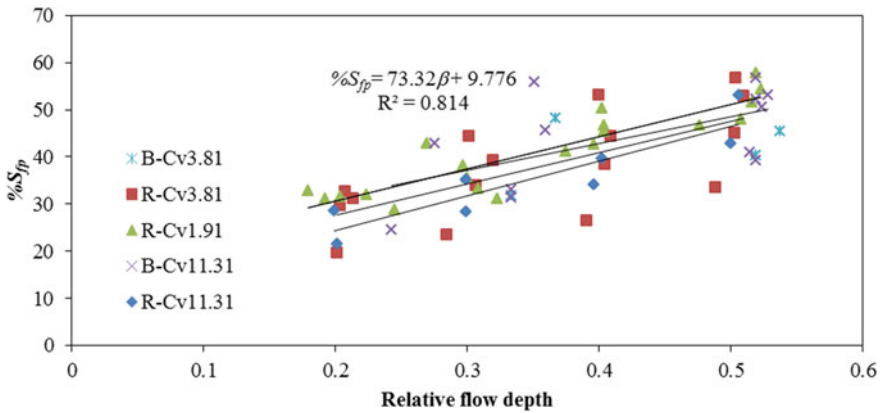


Fig. 11.3 Variation of  $\%S_{fp}$  with relative flow depth for converging compound channel

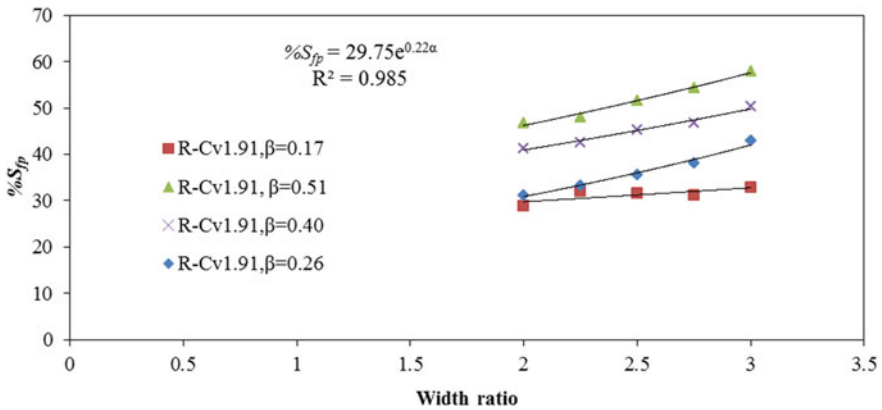


Fig. 11.4 Variation of  $\%S_{fp}$  with width ratio for converging compound channel



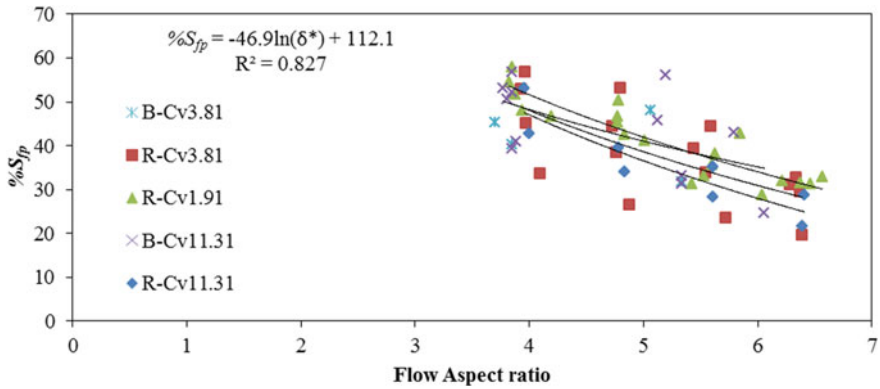


Fig. 11.5 Variation of  $\%S_{fp}$  with flow aspect ratio for converging compound channel

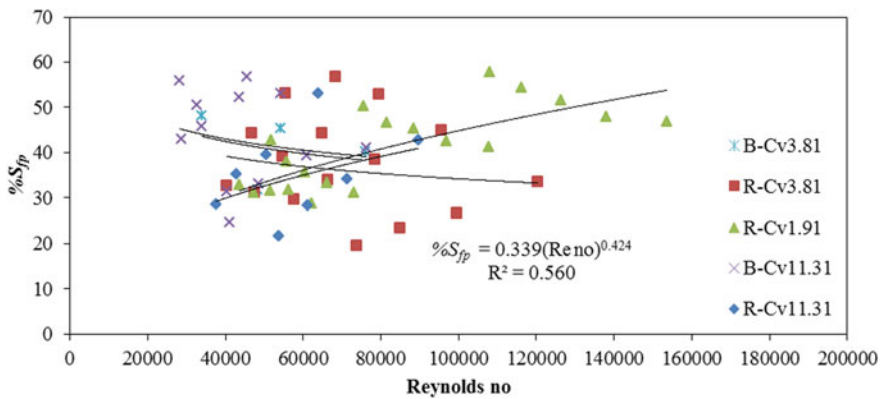


Fig. 11.6 Variation of  $\%S_{fp}$  with Reynolds number for converging compound channel

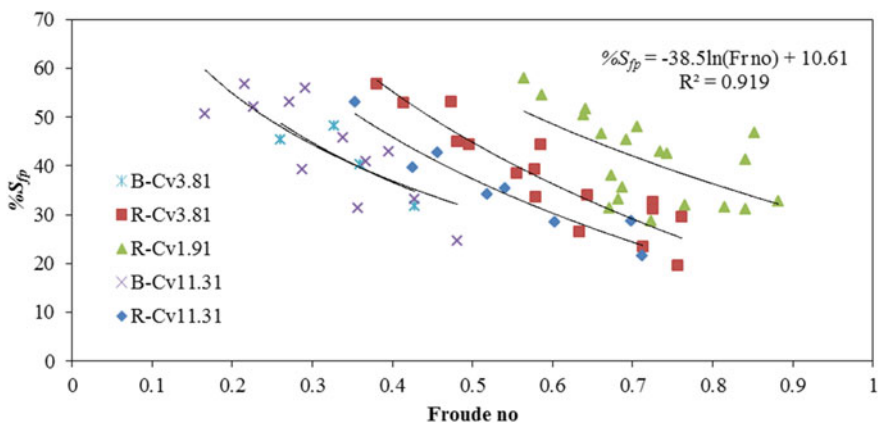


Fig. 11.7 Variation of  $\%S_{fp}$  with Froude number for converging compound channel

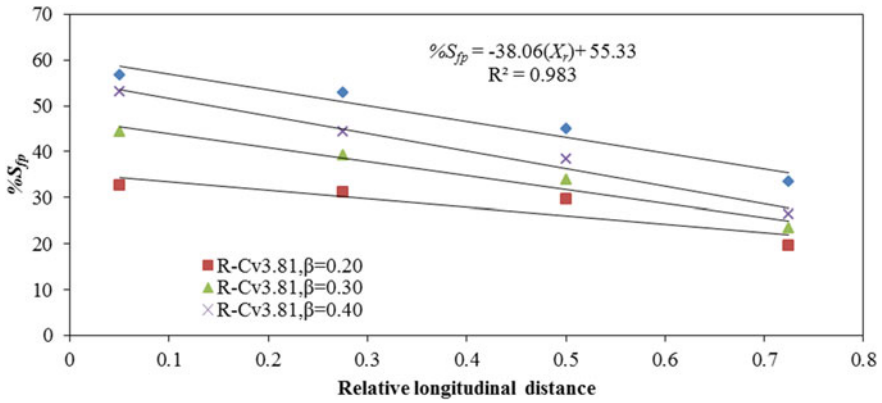


Fig. 11.8 Variation of  $\%S_{fp}$  with relative longitudinal distance for converging compound channel

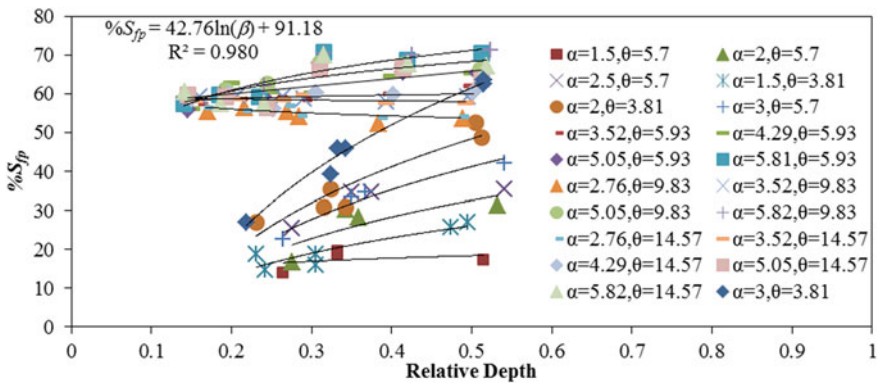


Fig. 11.9 Variation of  $\%S_{fp}$  with relative flow depth for diverging compound channel

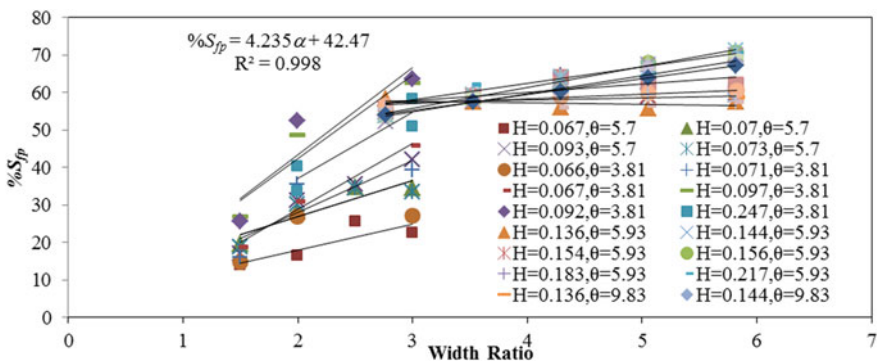


Fig. 11.10 Variation of  $\%S_{fp}$  with width ratio for diverging compound channel

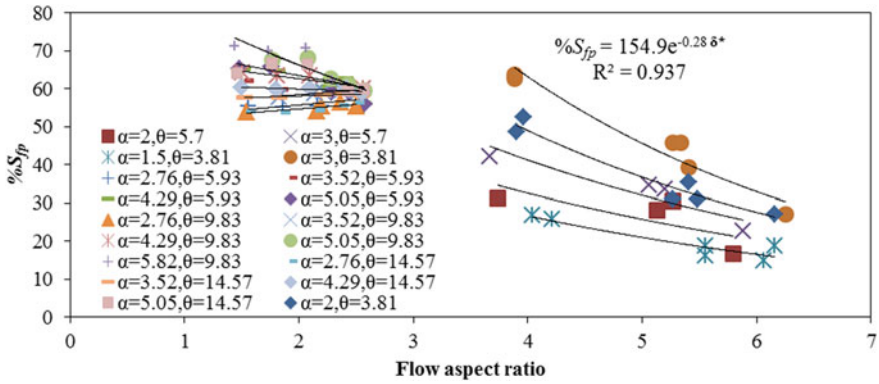


Fig. 11.11 Variation of  $\%S_{fp}$  with flow aspect ratio for diverging compound channel

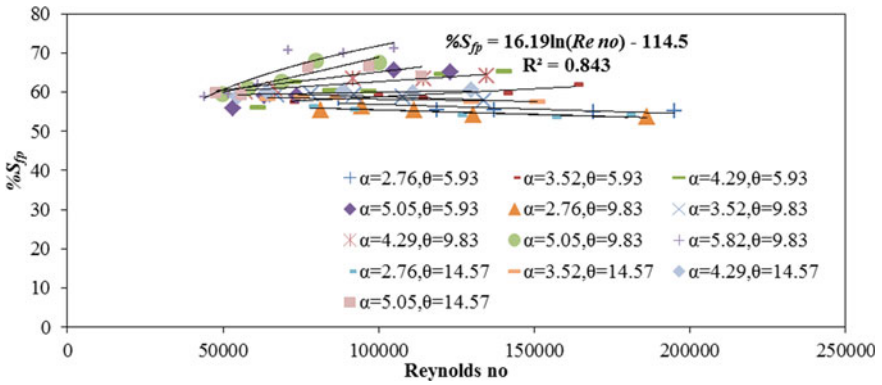


Fig. 11.12 Variation of  $\%S_{fp}$  with Reynolds number for diverging compound channel

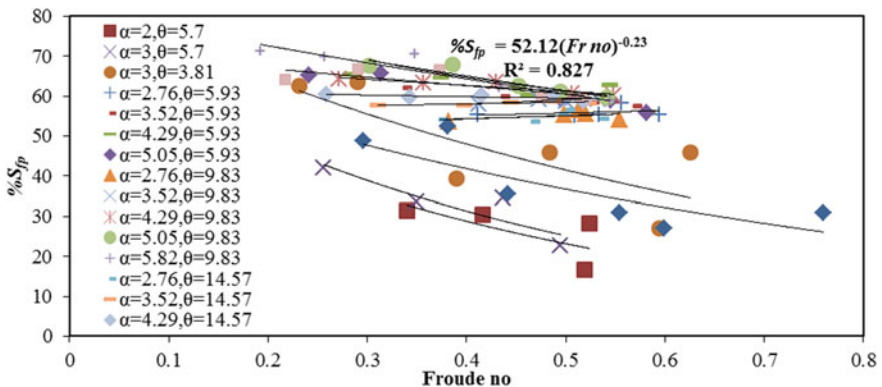


Fig. 11.13 Variation of  $\%S_{fp}$  with Froude number for diverging compound channel

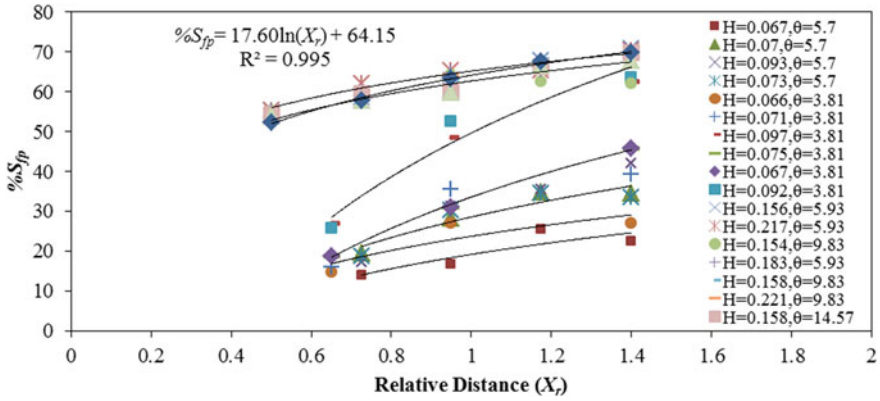


Fig. 11.14 Variation of %S<sub>fp</sub> with relative distance for diverging compound channel

existing between the %S<sub>fp</sub> with α, β, δ\*, Re, Fr, X<sub>r</sub> are logarithmic, linear, exponential, logarithmic, power, and logarithmic, respectively, for all diverging compound channel considered.

### 11.3.2 Formulation of the Multi-variable Regression Model

Six numbers of possible single regression models between dependent parameter and independent parameters are selected with highest coefficient of determination (R<sup>2</sup>). Based on the relationships obtained by analyzing the large numbers of published data sets, individual formulations have now been developed using multi-variable regression analysis. Compiling all the individual relationships two generalized formulae are developed for converging and diverging compound channels. Finally, the models of %S<sub>fp</sub> with high coefficient of determination (R<sup>2</sup>) of 0.90 are obtained.

For converging compound channels

$$\%S_{fp} = -188 + 40e^{0.22\alpha} + 148\beta + 59\ln\delta^* + 0.0634Re\ no^{0.424} - 2.28\ln(Fr\ no) + 6.63X_r \tag{11.3}$$

For diverging compound channels

$$\%S_{fp} = 223 + 3.32\alpha + 11.15\ln\beta + 113e^{-0.28\delta^*} - 11.35\ln Re\ no - 79Fr\ no^{-0.23} + 3.52\ln X_r \tag{11.4}$$

The resulted equation of percentage shear force on floodplains %S<sub>fp</sub> has now been applied to both non-prismatic data sets of previous investigators. Figure 11.15 demonstrates the predicted %S<sub>fp</sub> verses the experimental %S<sub>fp</sub> values for various

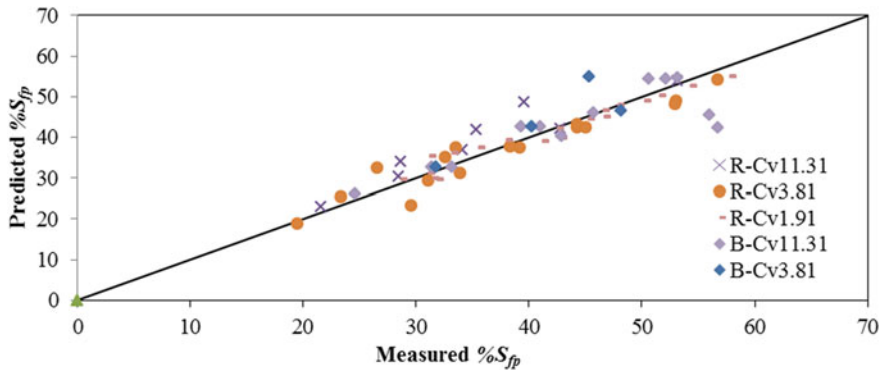


**Fig. 11.15** Comparison of predicted  $%S_{fp}$  with experimental predicted  $%S_{fp}$  for various converging compound channels

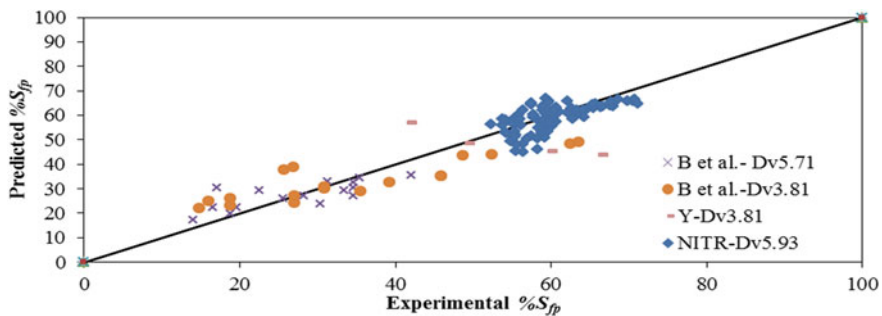


**Fig. 11.16** Comparison of predicted  $%S_{fp}$  with experimental predicted  $%S_{fp}$  for various diverging compound channels

converging compound channels. Similarly Fig. 11.16 demonstrates the predicted  $%S_{fp}$  versus the experimental  $%S_{fp}$  values for different diverging compound channels. These figures indicate the good agreement of models results with their actual values as they are very close to the line of good agreement.

The above expressions, i.e., Eqs. (11.3) and (11.4), are used for successfully estimating the percentage shear force on floodplain any selected location along the length of the channel where the six independent non-dimensional parameters are known. The efficiency of the models shows that they can be applied in natural rivers with minimum errors. For determining the water surface profile in converging compound channels, the equation developed by Rezaei (2006) can be used.

## 11.4 Conclusions

It is observed from the experimental data sets that the variations of flow variables along the stream-wise direction for narrowing and enlarging floodplains are not similar. So, individual models for percentage boundary shear force in floodplains have been proposed for such channels through multi-variable regression model. The models are expressed in terms of non-dimensional parameters such as width ratio, relative flow depth, flow aspect ratio, Reynolds number, Froude number, and relative longitudinal distance. These models will be helpful in accounting the apparent shear stress at the interface. The magnitudes of apparent shear stress at the interface are enumerated for both the converging and diverging compound channels. The applicability of the model is verified against the published data sets of previous investigators.

## References

- Bousmar D, (2002) Flow modelling in compound channels, momentum transfer between main channel and prismatic or non-prismatic floodplains. *Unité de Génie Civil et Environnemental* 326
- Bousmar D, Zech Y (1999) Momentum transfer for practical flow computation in compound channels. *J Hydraul Eng* 125(7):696–706
- Bousmar D, Wilkin N, Jacquemart JH, Zech Y (2004) Overbank flow in symmetrically narrowing floodplains. *J Hydraul Eng* 130(4):305–312
- Das BS, Khatua KK (2018) Flow resistance in a compound channel with diverging and converging floodplains. *J Hydraul Eng* 144(8):04018051
- Das BS, Devi K, Khatua KK (2019) Prediction of discharge in converging and diverging compound channel by gene expression programming. *ISH J Hydraulic Eng* 1–11
- Das BS, Devi K, Khuntia JR, Khatua KK (2020) Discharge estimation in converging and diverging compound open channels by using adaptive neuro-fuzzy inference system. *Can J Civ Eng* 47(12):1327–1344
- Devi K, Khatua KK (2019) Discharge prediction in asymmetric compound channels. *J Hydro-Environ Res* 23:25–39
- Devi K, Khatua KK (2020, December). Boundary shear distribution in a compound channel with differential roughness. In: *Proceedings of the institution of civil engineers-water management*, vol 173, no 6. Thomas Telford Ltd, pp 274–292
- Devi K, Khatua KK, Khuntia JR (2017) Boundary shear stress distribution for a two-stage asymmetric compound channel. *Arab J Sci Eng* 42(3):1077–1091
- Khatua KK, Patra KC (2007) Boundary shear stress distribution in compound open channel flow. *ISH J Hydraulic Eng* 13(3):39–54
- Khatua KK, Patra KC, Mohanty PK (2011) Stage-discharge prediction for straight and smooth compound channels with wide floodplains. *J Hydraul Eng* 138(1):93–99
- Khatua KK, Patra KC, Mohanty PK (2012) Stage-Discharge Prediction for Straight and Smooth Compound Channels with Wide Floodplains. *J Hydraulic Eng* 138(1):93–99. [https://doi.org/10.1061/\(ASCE\)HY.1943-7900.0000491](https://doi.org/10.1061/(ASCE)HY.1943-7900.0000491)
- Khuntia JR, Devi K, Khatua KK (2018) Boundary shear stress distribution in straight compound channel flow using artificial neural network. *J Hydrol Eng* 23(5):04018014
- Knight DW, Demetriou JD (1983) Flood plain and main channel flow interaction. *J Hydraul Eng* 109(8):1073–1092

- Knight DW, Hamed ME (1984) Boundary shear in symmetrical compound channels. *J Hydraul Eng* 110(10):1412–1430
- Mohanty PK (2013) Flow analysis of compound channels with wide flood plains. Doctoral dissertation, NIT Rourkela, India
- Mohanty PK, Khatua KK (2014) Estimation of discharge and its distribution in compound channels. *J Hydrodyn Ser B* 26(1): 144–154
- Naik B, Khatua KK (2016) Boundary shear stress distribution for a converging compound channel. *ISH J Hydraulic Eng* 22(2):212–219
- Naik B, Khatua KK, Wright NG, Sleigh A (2017) Stage-discharge prediction for converging compound channels with narrow floodplains. *J Irrig Drain Eng* 143(8):04017017
- Proust S (2005) Ecoulements non-uniformes en lits composés: effets de variations de largeur du lit majeur. Doctoral dissertation, Ph.D. thesis, INSA Lyon, Lyon, France, 362 p. <http://cemadoc.cemagref.fr/cemoa/PUB00018439>
- Proust S, Riviere N, Bousmar D, Paquier A, Zech Y, Morel R (2006) Flow in compound channel with abrupt floodplain contraction. *J Hydraulic Eng* 132(9):958–70
- Proust S, Fernandes JN, Peltier Y, Leal JB, Riviere N, Cardoso AH (2013) Turbulent non-uniform flows in straight compound open-channels. *J Hydraul Res* 51(6):656–667
- Rezaei B, (2006) Overbank flow in compound channels with prismatic and non-prismatic floodplains. Doctoral dissertation, University of Birmingham, UK
- Rezaei B, Knight DW (2009) Application of the Shiono and Knight Method in compound channels with non-prismatic floodplains. *J Hydraul Res* 47(6):716–726
- Yonesi HA, Omid MH, Ayyoubzadeh SA (2013) The hydraulics of flow in non-prismatic compound channels. *J Civil Eng Urban* 3(6):342–356